

AD-A051 887

UTAH UNIV SALT LAKE CITY DEPT OF CHEMISTRY
BRILLOUIN SCATTERING AND SEGMENTAL MOTION OF A POLYMERIC LIQUID--ETC(U)
MAR 78 Y LIN, C H WANG

F/G 11/9

N00014-75-C-0908

UNCLASSIFIED

TR-16

NL

| OF |

AD
A051 887



END

DATE

FILMED

5-78

DDC

Unclassified

SECURITY CLASSIFICATION OF THIS PAGE (When Data Entered)

REPORT DOCUMENTATION PAGE

READ INSTRUCTIONS
BEFORE COMPLETING FORM

1. REPORT NUMBER 14-TR-16		2. GOVT ACCESSION NO.	3. RECIPIENT'S CATALOG NUMBER
4. TITLE (and Subtitle) Brillouin Scattering and Segmental Motion of a Polymeric Liquid, II,		5. TYPE OF REPORT & PERIOD COVERED Technical (rept.)	
7. AUTHOR(s) Y.-H. Lin and C. H. Wang		8. CONTRACT OR GRANT NUMBER(s) N00014-75-C-0908	
9. PERFORMING ORGANIZATION NAME AND ADDRESS Department of Chemistry University of Utah Salt Lake City, UT 84112		10. PROGRAM ELEMENT, PROJECT, TASK AREA & WORK UNIT NUMBERS NR 051-562	
11. CONTROLLING OFFICE NAME AND ADDRESS		12. REPORT DATE 1 March 1, 1978	
		13. NUMBER OF PAGES 12-134 p. 1 26	
14. MONITORING AGENCY NAME & ADDRESS (if different from Controlling Office)		15. SECURITY CLASS. (of this report) Unclassified	
		15a. DECLASSIFICATION/DOWNGRADING SCHEDULE	
16. DISTRIBUTION STATEMENT (of this Report) a. According to the attached distribution list b. Others may obtain copies of this report from the Office of Technical Services, Department of Commerce.			
17. DISTRIBUTION STATEMENT (of the abstract entered in Block 20, if different from Report)			
18. SUPPLEMENTARY NOTES To be published in Molecular Physics			
19. KEY WORDS (Continue on reverse side if necessary and identify by block number) Brillouin scattering, viscous polymer fluid, polyethylene glycol, structural relaxation, hypersonic attenuation, segmental motion in polymers.			
20. ABSTRACT (Continue on reverse side if necessary and identify by block number) We have studied the Brillouin scattering spectra of oligomers of polyethylene glycol, along with ethylene glycol. These systems vary greatly in viscosity as well as molecular weight. We have found that except for ethylene glycol (the monomer), the Brillouin frequencies and the linewidths of the rest of oligomers show more or less the same temperature dependence, independent of viscosity and molecular weight. These results indicate that the motion responsible for the hypersonic dispersion and attenuation is localized. We have also developed a theory based upon the Zwanzig-Mori formalism to account for			

DD FORM 1 JAN 73 1473 EDITION OF 1 NOV 65 IS OBSOLETE

DISTRIBUTION STATEMENT A

Approved for public release;
Distribution Unlimited

400 730

AD A051887

AD NO. _____
DDC FILE COPY

DDC
MAR 30 1978
F

TC

the experimental results. We have then shown that in order to obtain a good agreement between theory and the experiment, the usual Markov approximation describing the dynamic behavior of the memory function cannot be used. Thus, the usual hydrodynamic equations with frequency independent transport coefficients are inadequate in describing the Brillouin scattering spectra of viscous liquids.

ACCESSION for	
NTIS	W. H. Section <input checked="" type="checkbox"/>
DDC	B. H. Section <input type="checkbox"/>
UNANNOUNCED	<input type="checkbox"/>
JUL 1 1961	
BY	
DISTRIBUTION/AVAILABILITY CODES	
A	

OFFICE OF NAVAL RESEARCH

Contract N00014-75-C-0908

Task No. NR 051-562

TECHNICAL REPORT NO. 16

BRILLOUIN SCATTERING AND SEGMENTAL MOTION
OF A POLYMERIC LIQUID, II

by

Y.-H. Lin and C. H. Wang

Prepared for Publication

in the

Molecular Physics

Department of Chemistry
University of Utah
Salt Lake City, Utah 84112

March 1, 1978

Reproduction in whole or in part is permitted for any purpose of the
United States Government

Approved for Public Release; Distribution Unlimited

Brillouin Scattering and Segmental
Motion of a Polymeric Liquid, II

by

Y.-H. Lin, C. H. Wang and D. R. Jones[†]
Department of Chemistry
University of Utah
Salt Lake City, Utah 84112
U.S.A.

[†]Present Address:

Department of Chemistry
California Polytechnic State University
San Luis Obispo, California 93407

Abstract

We have studied the Brillouin scattering spectra of oligomers of polyethylene glycol, along with ethylene glycol. These systems vary greatly in viscosity as well as molecular weight. We have found that except for ethylene glycol (the monomer), the Brillouin frequencies and the linewidths of the rest of oligomers show more or less the same temperature dependence, independent of viscosity and molecular weight. These results indicate that the motion responsible for the hypersonic dispersion and attenuation is localized. We have also developed a theory based upon the Zwanzig-Mori formalism to account for the experimental results. We have then shown that in order to obtain a good agreement between theory and the experiment, the usual Markov approximation describing the dynamic behavior of the memory function cannot be used. Thus, the usual hydrodynamic equations with frequency independent transport coefficients are inadequate in describing the Brillouin scattering spectra of viscous liquids.

Introduction

Modern development in optical technology has made the Rayleigh and Brillouin light scattering technique very useful for the investigation of molecular dynamic properties of large molecules such as polymers.¹⁻⁴ In general, the Rayleigh and depolarized Rayleigh measurements yield information on the translational and rotational diffusive motions of molecular segments and an entire molecule.¹ On the other hand, Brillouin scattering is due to the interaction of incident light with thermally induced sound waves in the medium and thus reflects the cooperative motion among different segments and molecules.⁵ Therefore the interaction between different molecules and segments is expected to have an important effect on the Brillouin scattering spectrum of a polymer fluid.

We have previously reported the Brillouin scattering results of polypropylene glycol (PPG).^{2,3,5} From these experimental results, we have come to believe that the molecular dynamics which can affect Brillouin spectra of polymeric liquids are localized motion involving only very few segments. In order to further affirm these results, we have carried out a systematic investigation of the Brillouin spectra of low molecular weight oligomeric polyethylene glycol (PEG) liquids including ethylene glycol. The experimental setup for such studies was similar to that used for the PPG measurement.^{2,3} We have also carried out viscosity measurements and compared the Brillouin scattering results with the classical theory on the sound propagation and attenuation. We have found that classical theory is not adequate for PEG. The viscosities of bulk polymer fluids such as PPG and PEG are

much higher than those of ordinary simple liquids. This is due to strong intermolecular interactions among segments, which render these polymer fluids highly viscous. In a previous paper⁵ we have used the Zwanzig-Mori linear response theory to analyze the Brillouin scattering results of bulk liquid polypropylene glycols (PPG). It was shown that the second moment of the intersegmental interaction potential and its relaxation dynamics have a dominant effect on the linewidth and frequency shift of the Brillouin peak.

In the present paper, we carry out a similar analysis for polyethylene glycol (PEG) liquids. To our knowledge the experimental Brillouin scattering results of these fluids have not been reported in the literature. We have presented the theoretical result more completely here than in the earlier paper. The derivation is carried out in terms of two coupled variables (density and velocity; or their linear combinations). Under certain approximations the final result in the present paper reduces to the previous one (Eq. (26) of Ref. 5), with which the PPG Brillouin scattering results were analyzed. The simplified equation is used to analyze the experimental Brillouin scattering results of PEG. The least squares fitting of PEG MW 200 to the theoretical expression was carried out. The result was found to be similar to that of PPG MW 425 as shown in the previous paper.

The measured sound velocity and attenuation coefficient results of the Brillouin scattering spectra of PEG dimer, trimer and oligomers of average molecular weights of 200 and 400 are shown together with that of ethylene glycol monomer in Figs. 1 and 2. The results indicate that Brillouin data show significant dispersion near 290 K. The Brillouin scattering result of the monomer is quite different from

the former group of PEG, whose Brillouin scattering results are found virtually independent of molecular weight. The cause for this difference is discussed. We have compared the Brillouin scattering results of the PPG with the PEG series, and have found a significant difference between them. This difference is interpreted as due to their different segmental mass and different degree of intermolecular interactions.

Theoretical Consideration

For a polymer liquid made up of a collection of identical chain segments, the isotropic part of the polarized Brillouin-Rayleigh spectrum observed at scattering angle θ is determined by the Fourier transform of the time correlation function of density fluctuations, given by

$$C_{\rho\rho}(\underline{q}, t) = \langle \delta\rho(\underline{q}, t) \delta\rho^*(\underline{q}) \rangle \quad (1)$$

where $\delta\rho(\underline{q}, t)$ is the \underline{q} th mode of the fluctuation of density and is given by

$$\delta\rho(\underline{q}, t) = \sum_j e^{i\underline{q} \cdot \underline{r}_j(t)} \quad (2)$$

Here $\underline{r}_j(t)$ is the position of scatterer (we take it to be a chain segment) at time t , \underline{q} is the scattering wave vector and is related to the wave vectors of incident and scattering light by

$$\underline{q} = \underline{K}_s - \underline{K}_i \quad (3)$$

In Eq. (2) the summation over j is to include all scatterers within the scattering volume.

In order to describe the Brillouin spectrum, we need to consider $V(\underline{q}, t)$ in addition to the density fluctuation $\delta\rho(\underline{q}, t)$. Here $V(\underline{q}, t)$ is

given by

$$\underline{V}(\underline{q}, t) = \sum_j \underline{V}_j e^{i\underline{q} \cdot \underline{r}_j(t)} \quad (4)$$

where \underline{V}_j is the velocity of segment j . If we choose \underline{q} to be in the direction of the z -axis of the laboratory coordinate system; then by symmetry only the z -component of $\underline{V}(\underline{q}, t)$ can couple to $\delta\rho(\underline{q}, t)$. In principle we need to consider the energy fluctuation to account for the dynamics of density fluctuations properly, but the inclusion of the energy fluctuation can only affect the Brillouin spectrum in minor ways (one of which is to render the hypersonic wave to propagate with an adiabatic velocity, rather than with an isothermal velocity, as considered in this paper). A complete microscopic theory on Brillouin scattering including the energy fluctuation is presently in progress.

The q th mode of density fluctuations when coupled to $V_z(q)$ will give rise to two Brillouin peaks in the Brillouin-Rayleigh spectrum. The two are the Stokes and anti-Stokes peaks associated with the longitudinal hypersonic wave. As shown in a previous paper, the two Brillouin peaks can be calculated by using the Zwanzig-Mori equation⁶ using two dynamic variables ξ_+ and ξ_- , which are defined as

$$\xi_{\pm} = \frac{1}{\sqrt{2}} \left(\frac{\delta\rho}{\langle |\delta\rho|^2 \rangle} \pm \frac{V_z}{\langle |V_z|^2 \rangle} \right) \quad (5)$$

where for the simplicity of notation we have suppressed the arguments associated with ξ_{\pm} , $\delta\rho$ and V_z , understanding that they all depend on both \underline{q} and t .

It is easy to show by using time reversal symmetry that at $t=0$, $\langle \xi_+ \xi_+^* \rangle = \langle \xi_- \xi_-^* \rangle = 1$ and $\langle \xi_+ \xi_-^* \rangle = \langle \xi_- \xi_+^* \rangle = 0$.

In the previous paper, we neglected the dynamic coupling between ξ_+ and ξ_- and treated only the motion of ξ_+ and ξ_- as independent variables. In this paper we take this coupling into account, and for this purpose, we define a column vector \underline{A} consisting of ξ_+ and ξ_- as its elements

$$\underline{A} = \begin{pmatrix} \xi_+ \\ \xi_- \end{pmatrix} \quad (6)$$

The equation of motion for $\underline{A}(t)$ is given formally by the Liouville equation,

$$\frac{\partial}{\partial t} \underline{A}(t) = iL\underline{A}(t) \quad (7)$$

where L is the classical Liouville operator governing the time evolution of the dynamic vector variable $\underline{A}(t)$. While it is straightforward to write down a formal expression for L in terms of the kinetic and potential energy operators in a many body system, in practice this is seldom done in a polymer system due to its large number of internal degrees of freedom and the intermolecular and intramolecular potential functions. Thus we shall utilize only the formalistic symmetry properties of the Liouville operator such as the time reversal, reflection and translation symmetry properties, instead of writing out its explicit form. In its formal definition the Liouville operator is self-adjoint.

For the set of dynamic variables $\underline{A}(t)$, the Mori transformation of Eq. (7) gives.

$$\frac{\partial}{\partial t} \underline{A}(t) = i\Omega \underline{A}(t) - \int_0^t d\tau \underline{K}(\tau) \cdot \underline{A}(t-\tau) + \underline{F}(t) \quad (8)$$

where the frequency matrix Ω is given in terms of L

$$\Omega = \langle (LA) A^+ \rangle \quad (9)$$

The other quantities are

$$K(\tau) = \langle F(\tau) F^+ \rangle \quad (10)$$

$$F(\tau) = e^{iQL\tau} F \quad (11)$$

$$F = iQLA \quad (12)$$

where $Q = (1-p)$, p being the Zwanzig-Mori projection operator defined as

$$pG = \langle GA^+ \rangle \langle AA^+ \rangle^{-1} A = \langle GA^+ \rangle A \quad (13)$$

due to the fact that $\langle AA^+ \rangle$ is a unit matrix.

Substituting Eq. (6) into Eq. (9), we obtain in the limit of small q ,

$$\Omega = \begin{pmatrix} \omega_q & 0 \\ 0 & -\omega_q \end{pmatrix} \quad (14)$$

where $\omega_q^2 = q^2 \frac{\langle |Vz|^2 \rangle}{\langle |\delta\rho|^2 \rangle} = q^2 (\rho m \chi_T)^{-1} = q^2 C_T^2$. Here χ_T is the isothermal compressibility and is related to $\langle |\delta\rho|^2 \rangle$ by

$$\langle |\delta\rho|^2 \rangle = V \rho^2 k T \chi_T \quad (15)$$

as $q \rightarrow 0$. C_T is the isothermal sound velocity.¹

Equation (14) thus indicates that $A(t)$ propagates with the isothermal sound velocity, instead of the desired adiabatic sound velocity. The reason for this is that, as mentioned above, we have not included the energy fluctuation term in the calculation. Since we shall at the end treat ω_q as a parameter to fit the experimental data, the omission of the coupling of density to energy will not affect the

interpretation of the Brillouin data to be given in the next section.

The matrix $K(\tau)$ is known as the memory function matrix. Upon the substitution of Eqs. (5) and (6) into Eq. (10) and after carrying out the necessary matrix multiplication, we find for the memory function,

$$\underset{\sim}{K}(\tau) = \begin{pmatrix} K(\tau) & -K(\tau) \\ -K(\tau) & K(\tau) \end{pmatrix} \quad (16)$$

where for small q

$$K(\tau) = \frac{1}{2} \{ \langle [e^{iL\tau} (iLV)] [iLV]^\star \rangle - \omega_q^2 \} \quad (17)$$

For brevity we have used V for V_z , and $e^{iL\tau}$ for $e^{iQL\tau}$. The latter simplification is possible for $q \rightarrow 0$.¹ At $\tau = 0$ it has been shown in Appendix II of Ref. 5 that $K(0)$ in the small q limit has the analytical form:

$$K(0) = \frac{1}{2} \left\{ \frac{q^2}{2Nm} \sum_i \sum_j \left\langle \frac{\partial^2 U}{\partial (Z_i - Z_j)^2} (Z_i - Z_j)^2 \right\rangle + \frac{3kT}{m} q^2 - \omega_q^2 \right\} \quad (18)$$

where U is the total potential energy of the system. The first term of Eq. (18) can be shown to be positive and greater than ω_q^2 . One can easily recognize that this term is proportional to the spatial second moment of the intermolecular and intersegmental potential energy in the Z direction.

Substitution of Eqs. (6), (14), and (16) into the generalized Langevin equation (Eq. (8)) gives two coupled kinetic equations:

$$\frac{\partial \xi_{\pm}}{\partial t}(t) = \pm \omega_q \xi_{\pm}(t) - \int_0^t [K(\tau) \xi_{\pm}(t-\tau) - K(\tau) \xi_{\mp}(t-\tau)] d\tau + F_{\pm}(t) \quad (19)$$

where $F_{\pm}(t)$ are the fluctuation forces acting on the slow variables $\xi_{\pm}(t)$. The two coupled kinetic equations can be solved by the method of Laplace transforms.

The memory function $K(\tau)$ is the time correlation function of fluctuation forces and should always decay to zero as time goes on. We have discussed in Ref. 5 that the time dependence of $K(\tau)$ can be approximated as an exponential decaying function with correlation time τ_R ,

$$K(\tau) = K(0) e^{-\frac{\tau}{\tau_R}} \quad (20)$$

we denote $\xi_{\pm}(s)$ and $K(s)$ as the Laplace transforms of $\xi_{\pm}(t)$ and $K(t)$ respectively, and also denotes

$$I_{\pm}(s) = \langle \xi_{\pm}(s) \xi_{\pm}^*(0) \rangle \quad (21)$$

$$I_{\pm\mp}(s) = \langle \xi_{\pm}(s) \xi_{\mp}^*(0) \rangle \quad (22)$$

From Eq. (1) and the definitions of ξ_{\pm} (Eq. (5)) one can show that the light scattering spectrum due to density fluctuation is

$$I(\omega) = \text{Re}_{s \rightarrow i\omega} [I_{+}(s) + I_{-}(s) + I_{+-}(s) + I_{-+}(s)]$$

where $\text{Re}_{s \rightarrow i\omega}$ denotes taking the real part after s is substituted by $i\omega$.

Solution of Eq. (19) using Eq. (20) for $K(\tau)$ yields the following results:

$$I(\omega) = I_{+}(\omega) + I_{-}(\omega) + I_{+-}(\omega) + I_{-+}(\omega) \quad (23)$$

$$I_{\pm}(\omega) = \frac{M - \Lambda_{\pm}}{[M - \Lambda_{\pm}]^2 + [\omega_{\mp}^2 - N - B_{\pm}]^2} \quad (24)$$

$$I_{\pm\mp}(\omega) = \frac{M^3 - M(\omega+\omega_q - N) - (\omega-\omega_q - N) - MN(\omega+\omega_q - N) - MN(\omega-\omega_q - N)}{Y_+ Y_-} \quad (25)$$

where

$$A_{\pm} = X_{\pm}/Y_{\pm} \quad (26)$$

$$B_{\pm} = \frac{(M^2 - N^2)(N - \omega \mp \omega_q) - 2M^2 N}{Y_{\pm}} \quad (27)$$

$$M = \frac{K(0)\tau_R}{1 + \omega^2 \tau_R^2} \quad (28)$$

$$N = \frac{K(0)\omega \tau_R^2}{1 + \omega^2 \tau_R^2} \quad (29)$$

$$X_{\pm} = (M^2 - N^2)M + 2MN(N - \omega \mp \omega_q) \quad (30)$$

$$Y_{\pm} = M^2 + (N - \omega \mp \omega_q)^2 \quad (31)$$

where M and N are the real and imaginary parts of $K(i\omega)$, respectively. In reaching the results of Eq. (25), we have neglected an unimportant term which appears in the denominators. Since the $I_{\pm\mp}(\omega)$ terms contribute much less to the total spectrum than the $I_{\pm}(\omega)$ terms, the neglect of the unimportant term in $I_{\pm\mp}(\omega)$ is justified as far as the calculation of the total Brillouin spectrum is concerned.

In the temperature region where $K\tau_R^2 \ll 1$ is valid, A_{\pm} and B_{\pm} terms of Eq. (24) are much smaller than the other terms, and $I_{\pm}(\omega)$ gives a maximum spectral intensity around $\omega = \pm(|\omega_q| + |N|)$. From Eq. (25) one notices that $I_{+-}(\omega)$ is identical to $I_{-+}(\omega)$. They give rise to a spectrum with a much broader bandwidth than that from $I_{\pm}(\omega)$. These terms have an intensity maximum centered at $\omega = 0$. However, the spectral wings of $I_{\pm\mp}(\omega)$ in the vicinity of $\omega = \pm(|\omega_q| + |N|)$ are negligible compared with $I_{\pm}(\omega)$.

The $I_{\pm}(\omega)$ terms as given in Eq. (25) represent the dynamic coupling of the two phonon modes with opposite velocity. This term is important to account for the shape of the entire Brillouin-Rayleigh spectrum, as it gives rise to a spectrum centered at zero frequency, as pointed out in the earlier paper.⁵ However, despite the presence of $I_{\pm}(\omega)$, we have found that $I_{\pm}(\omega)$, with the A_{\pm} and B_{\pm} terms neglected, provides an adequate account for the temperature dependences of the Brillouin linewidth and the frequency shift. The simplified spectral functions as given by the $I_{\pm}(\omega)$ terms were used to analyze the Brillouin data of PPG in the earlier paper. We now use the same spectral function, coupled with the least squares fitting procedure to analyze the PEG Brillouin scattering results.

Discussion of the Experimental

Results of PEG Brillouin Scattering

The measured Brillouin shift (f_B in Hertz) is related to the hypersonic velocity V_s by the equation:

$$V_s = f_B \lambda_o / 2n \sin(\frac{\theta}{2}) \quad (32)$$

where λ_o is the wavelength of the incident light in vacuum. n is the index of refraction of the scattering medium. θ is the scattering angle from the incident light. The attenuation coefficient ($\alpha\lambda_s$) over one wavelength of the hypersound is expressed as

$$\alpha\lambda_s = \pi \Gamma_B / f_B \quad (33)$$

where Γ_B is the instrument corrected Brillouin spectral full width at half-maximum intensity. λ_s is the wavelength of the hypersonic wave

and is given by

$$\lambda_s = \frac{V_s}{f_B} \quad (34)$$

The experimental results of V_s and $\alpha\lambda_s$ of ethylene glycol (monomer) and PEG dimer, trimer, and polymers of MW 200 and MW 400 at 90° scattering angle are presented in Figs. 1 and 2 as functions of temperature. Except for the ethylene glycol results, the $\alpha\lambda_s$ and V_s results for the other oligomers are virtually independent of molecular weight. As pointed out in the introduction, the same molecular weight independence was also observed for the PPG series.³ Since the Brillouin scattering spectrum of a viscous fluid is greatly influenced by the intermolecular and intersegmental interactions, the distinctive $\alpha\lambda_s$ results of ethylene glycol indicate that the dynamics of the intermolecular interaction of the monomer is quite different from the other members of the series. The difference is most likely due to its short molecular dimension and the presences of dominant hydrogen-bonding interaction with neighboring molecules.

Despite their different molecular weights, we have found that all of the PEG samples under the present study, have practically the same index of refraction (to within 1% of error). Thus, according to Eqs. (32) and (33), the same index of refraction implies that the Brillouin frequency shift and the linewidth are practically the same for all of the PEG samples of different molecular weights.

According to the Navier-Stokes equation, the hypersonic velocity depends only on adiabatic compressibility, and the attenuation coefficient (or linewidth) only on the static shear and bulk viscosities. For

the PEG system, the static shear viscosity changes markedly with temperature; the static bulk viscosity which is more or less proportional to the shear viscosity also changes rapidly with temperature. Thus the classical theory of sound propagation and attenuation cannot be used to describe the hypersonic propagation and attenuation behavior.

It is now recognized that the acoustical behavior of highly viscous liquids depends on the product of sound frequency and the viscosity (i.e., $f_B \eta$) and not on the parameters separately. For this reason, we have measured the viscosity of ethylene glycol and all of the members of PEG studied. We have plotted the hypersonic velocity (V) and attenuation coefficient ($\alpha\lambda$) as a function of $f_B \eta$ in Figs. (3) and (4) respectively. In terms of such plots, V and $\alpha\lambda$ separate into different curves for different PEG members, due to the fact that each member of PEG has a different viscosity at a given temperature. At a fixed $f_B \eta$, the monomer gives the largest V . However, the functional dependence of $\alpha\lambda$ on $f_B \eta$ is more complicated. At low $f_B \eta$ value ($f_B \eta < 150 \text{ GHz cp}$), corresponding to the high temperature situation, $\alpha\lambda$ is independent of molecular weight. Beyond this value $\alpha\lambda$ increases with increasing degree of polymerization, with some anomaly observed for the monomer result. The velocity data approach plateau values at large $f_B \eta$ for each oligomer, whereas $\alpha\lambda$ decreases gradually at large $f_B \eta$.

Doubtless to say, the $f_B \eta$ dependence of V and $\alpha\lambda$ is due to the structural relaxation effect taking place at the hypersonic frequency region in PEG. Assuming that the structural relaxation time is proportional to the shear viscosity, we have tried to interpret our results

according to a relaxation theory set forth by Leontovich,⁷ and found that the relaxation theory predicts too strong a dependence of V and $\alpha\lambda$ on $f_{B\eta}$ at large $f_{B\eta}$.

We thus fit, with the help of a least-squares program, the experimental results of the frequency shift and linewidth to the values generated from the spectral functions for Brillouin scattering as given in Eq. (24). Neglecting the A_{\pm} and B_{\pm} terms, we obtain from Eq. (24),

$$I(\omega) = \frac{M}{M^2 + [\omega - \omega_q - N]^2} + \frac{M}{M^2 + [\omega + \omega_q - N]^2} \quad (35)$$

In the least-squares fitting, we first generated the whole Brillouin spectrum using Eq. (35). The frequency shift of peak maximum and linewidth of the generated spectrum were then read and compared with the experimental values. The difference between the theoretical and experimental values is then minimized with the least-squares fitting program. The temperature dependence of the relaxation time τ_R associated with the memory function is assumed to follow the Arrhenius equation

$$\tau_R = \tau_R^{\circ} \exp (E_a/kT) \quad (36)$$

where E_a is the activation energy for the relaxation process of the second moment of intersegmental interaction potential.⁵ In the least-squares fitting program, there are three adjustable parameters: the initial value of memory function at $t = 0$, K ; the activation energy E_a ; and the relaxation time τ_R° at infinitely high temperature (see Eq. (36)). The result of the least-squares fitting is shown in Fig.

5, along with the experimental results.

The fittings were carried out in two cases: 1) ω_q independent of temperature and 2) ω_q a function of temperature. The latter case represents a more realistic situation. With ω_q fixed, the fitting to the linewidth data is excellent, however, there are deviations in the calculated frequency shifts from their experimental data at both high and low temperatures. As pointed out in the previous paper,⁵ ω_q , being proportional to $(m\rho\chi_T)^{-1/2}$, is temperature dependent and is larger at lower temperature. If the temperature dependence of ω_q is included, the calculated frequency shift values are significantly improved at both low and high temperatures. Since the functional form of the temperature dependence of ω_q is not available, to demonstrate this point, we simply assume that the temperature dependent function for ω_q is

$$\omega_q = \omega_q^\circ + \frac{m_1}{T} + \frac{m_2}{T^2} + \frac{m_3}{T^3} \quad (37)$$

where ω_q° is the value of ω_q at infinite high temperature, and m_1 , m_2 , and m_3 are adjustable parameters. Using Eq. (37), we have found that the fitting to the linewidth data is virtually unchanged, but the fitting to the frequency shift data becomes excellent at all temperatures. The improvement of the fitting to the frequency by allowing ω_q to be temperature dependent does not change the K , E_a and τ_R° values significantly. The obtained best values for these three parameters are $K = 13 \text{ (GHz)}^2$, $E_a = 4.11 \text{ kcal/mole}$ and $\tau_R^\circ = 1.56 \times 10^{-14} \text{ sec}$ for ω_q fixed, and $K = 14.2 \text{ (GHz)}^2$; $E_a = 3.58 \text{ kcal/mole}$ and $\tau_R^\circ = 3.0 \times 10^{-14} \text{ sec}$ for ω_q being temperature dependent. The difference in the values of activation energy is less than 15%, which is about the

order of the usual error in the activation energy measurement.

As in the least-squares fitting of the PPG data, the obtained K value is a fraction of ω_q^2 . However, the activation energy, E_a , is found slightly smaller than that of PPG.⁵ Qualitatively this is expected, since PPG has an extra methyl group for the side chain, which will increase the hindrance against the motion of each segment. Nevertheless, the general characteristics of the results obtained for PEG by the least-squares fitting are similar to those of PPG. Thus the discussion of the previous paper⁵ on PPG applies equally well to the present case.

A common feature of the PPG series studied in the previous paper and the PEG series of the present study is their large viscosities, compared with fluids composed of simple molecules. In Fig. 1 of the previous paper, we have shown that the Brillouin scattering results of the PPG samples are virtually independent of their viscosities. This is also the case for the PEG series. The high viscosity of the polymer fluid invalidates the Navier-Stokes equation used for the Newtonian fluids.⁸ As seen from our theoretical analysis, the memory function is characterized by the spatial second moment of interaction potential between segments and its relaxation dynamics. Due to the strong intersegmental interaction, the memory function cannot be replaced by a relaxation parameter multiplied by a delta function generally known as the Markov approximation. In the present theory, the convolution form of the memory function and the dynamic variables is preserved. This feature, although not well recognized, is believed to

be very important for describing the structural relaxation process taking place in the hypersonic frequency region. To be more specific, the imaginary part of the Fourier transform of the memory function (the N function given in Eq. (29)) is very important to account for the dispersion of the peak frequency, and the real part (M as given in Eq. (28)) for the maximum in the linewidth.

In Frenkel's hole theory of liquids,⁹ molecules are considered to move continuously into the vacancies which are proposed to exist in a viscous liquid. Based on this hole concept, Isakovich and Chaban¹⁰ have modeled the highly viscous liquid as a micro-inhomogeneous medium to explain the sound attenuation at the hypersonic frequency region. A micro-inhomogeneous medium is one which consists of two or more inhomogeneous regions, the dimensions of which are assumed to be small compared to the wavelength of sound. They have assumed that upon the passage of sound waves an exchange of energy between different regions in the micro-inhomogeneous medium occurs. The energy exchange is considered to be due to mutual diffusion of holes in different regions. Our present theoretical analysis does not assume such a model. It is shown that the initial value of the memory function is characterized by the spatial second moment of the intersegmental interaction potential. The rapid motion of a chain segment from one position to another is responsible for the decay of the memory function, and also causes a local reorganization of the structure in a polymer liquid. This microscopic picture is implied in Isakovich and Chaban's model of structural relaxation in a highly viscous liquid, but they do not include the memory effect in the calculation. The pre-

sent theory is developed on the basis of the Zwanzig-Mori formalism, and allows one easily to relate the phenomenological quantities in terms of a microscopic picture associated with the physical system under study with a minimum of subsidiary assumptions about the nature of the system. The present microscopic theory, thus, serves to provide the Isakovich and Chaban phenomenological theory with a more satisfactory statistical foundation.

Summary and Conclusion

We have studied the Brillouin spectra of PEG, along with ethylene glycol. These systems along with PPG vary greatly in viscosity as well as molecular weight. We have found that except for monomer, the Brillouin frequency and the linewidth of PEG are insensitive to viscosity and molecular weight. These results indicate that the motion responsible for the hypersonic dispersion and attenuation is localized. Despite some difference with respect to the temperature behavior in the relaxation time associated with memory function, the PEG results closely resemble those of PPG.

We have developed a theory on the basis of the Zwanzig-Mori formalism to account for the experimental results. We have then shown that in order to obtain a good agreement between theory and the experiment, the usual Markov approximation describing the dynamic behavior of the memory function cannot be used. Thus, the usual hydrodynamic equations with frequency independent transport coefficients are inadequate in describing Brillouin scattering of viscous liquids. Further studies of Brillouin scattering spector will definitely provide useful information about the dynamic structure of the liquid state.

Acknowledgment: We thank the Office of Naval Research and the National Science Foundation for financial support of this research.

References

1. B. J. Berne and R. Pecora, Dynamic Light Scattering (Wiley-Interscience, 1976).
2. Y. Y. Huang and C. H. Wang, J. Chem. Phys., 62, 120 (1974).
3. C. H. Wang and Y. Y. Huang, J. Chem. Phys., 64, 4748 (1976).
4. G. D. Patterson, J. Polymer Sci., Polymer Physics Ed., 15, 579 (1977).
5. Y.-H. Lin and C. H. Wang, (submitted for publication).
6. H. Mori, Prog. Theor. Phys. (Kyoto) 33, 423 (1965); 34, 399 (1965) and references cited therein.
7. M. A. Leontovich and L. I. Mandel'shtam, JETP 7, 438 (1937).
8. R. D. Mountain, J. Res. N.B.S. 70A, 207 (1966); 72A, 75 (1968); CRSS 1, 5 (1970).
9. J. I. Frenkel, Kinetic Theory of Liquids (Oxford University Press, Oxford, 1946).
10. M. A. Isakovich and I. A. Chaban, Sov. Phys. -JETP, 23, 893 (1966).

Figure Captions

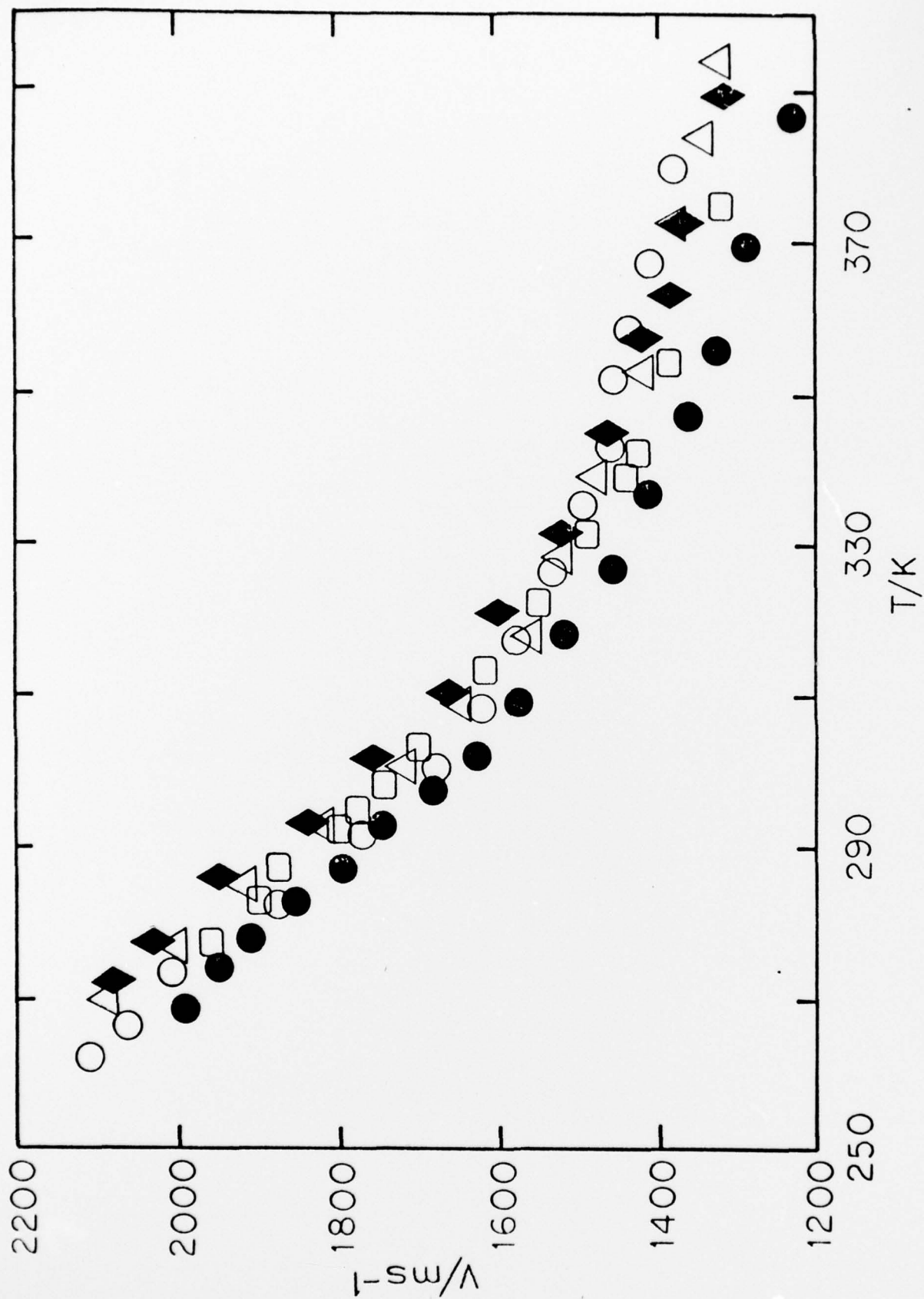
Figure 1. Hypersonic velocities of ethylene glycol (\circ) and PEG dimer (Δ), trimer (\diamond), MW 200 (\bullet) and MW 400 (\square) as a function of temperature.

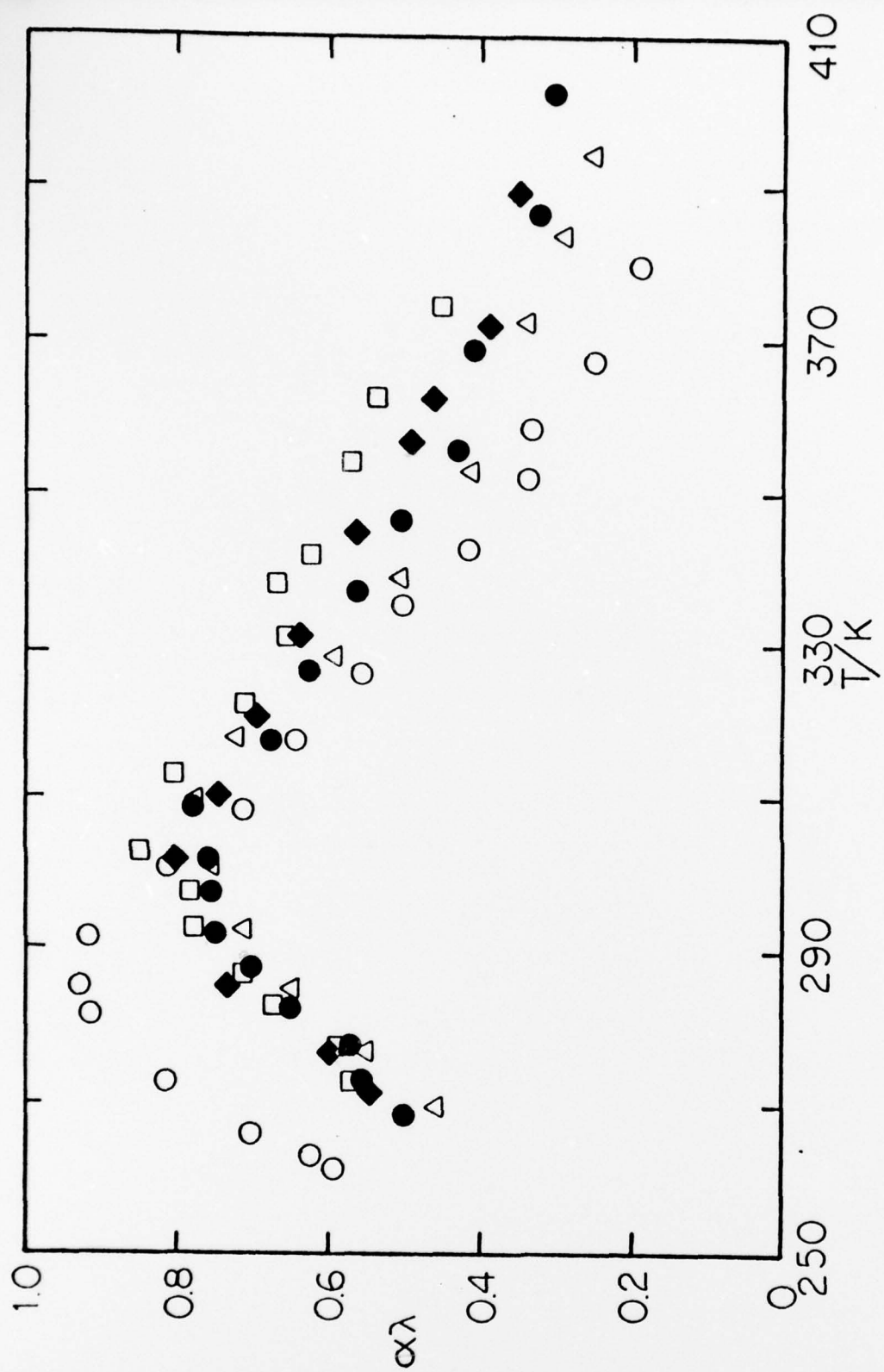
Figure 2. Hypersonic attenuation coefficients as a function of temperature (symbols are the same as those in Fig. 1).

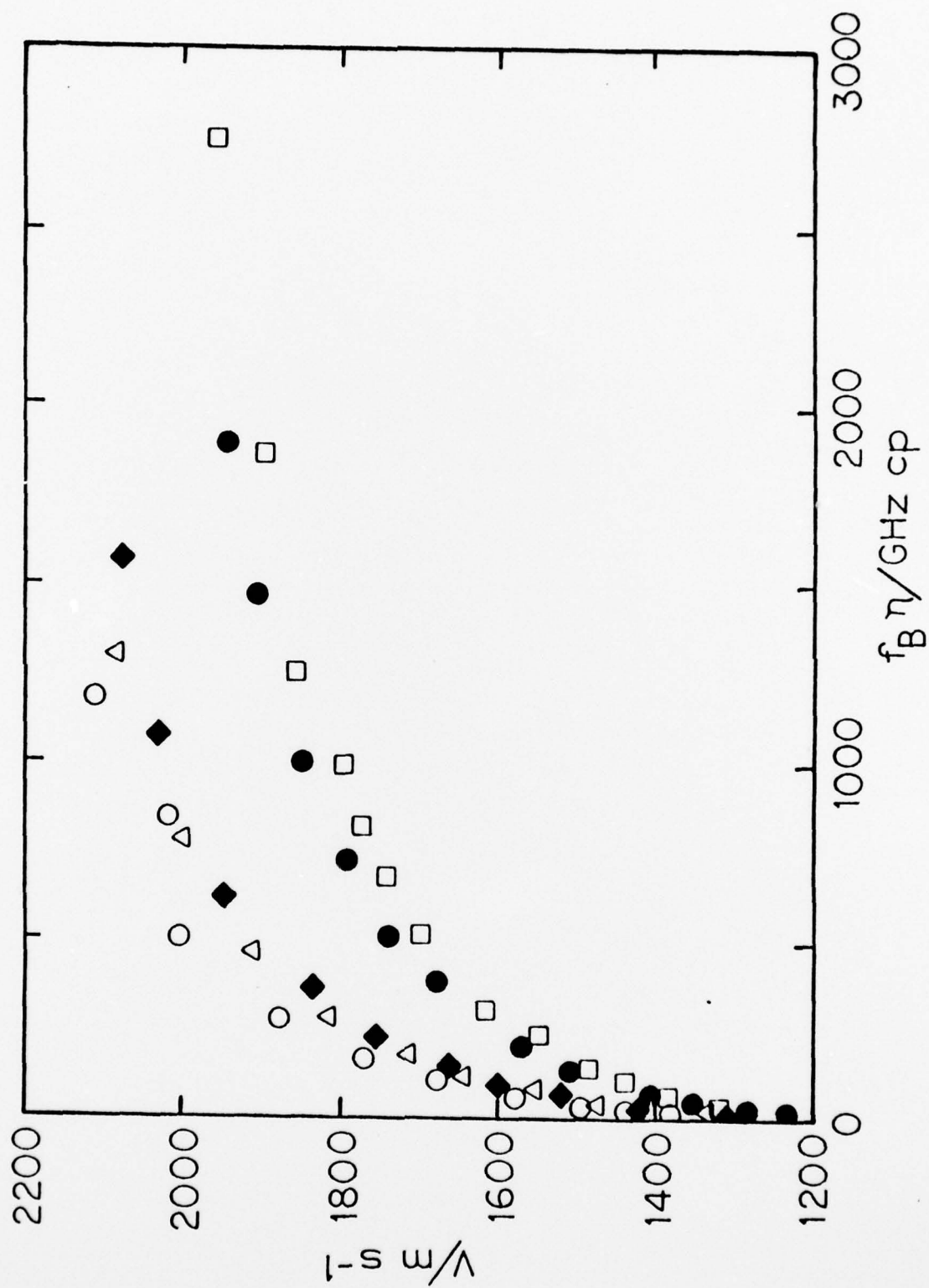
Figure 3. Hypersonic velocities as a function of $f_B \eta$ (f_B is the hypersonic frequency and η the shear viscosity; other symbols are the same as those in Fig. 1).

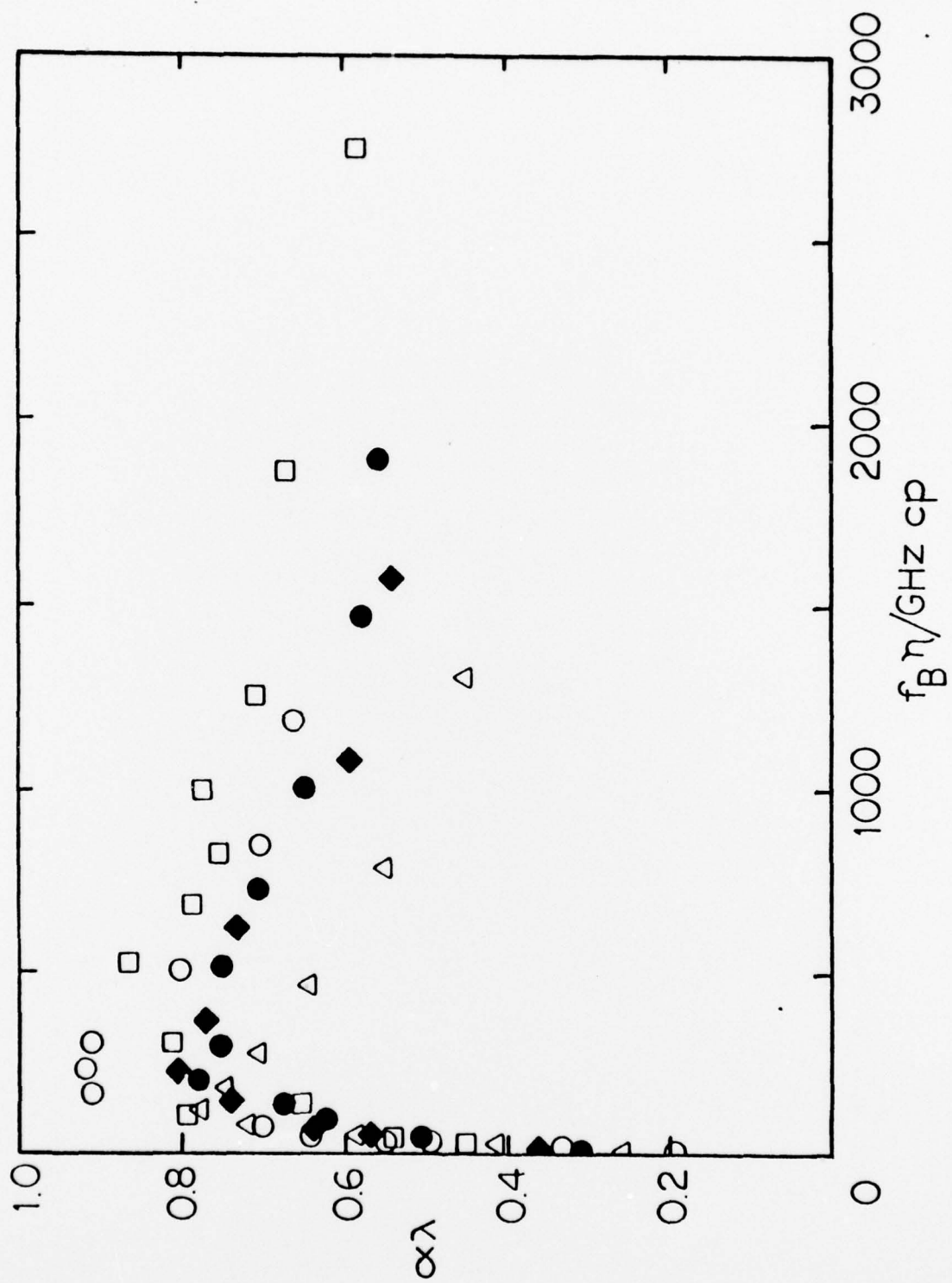
Figure 4. Hypersonic attenuation coefficients as a function of $f_B \eta$ (symbols are the same as those in Fig. 3).

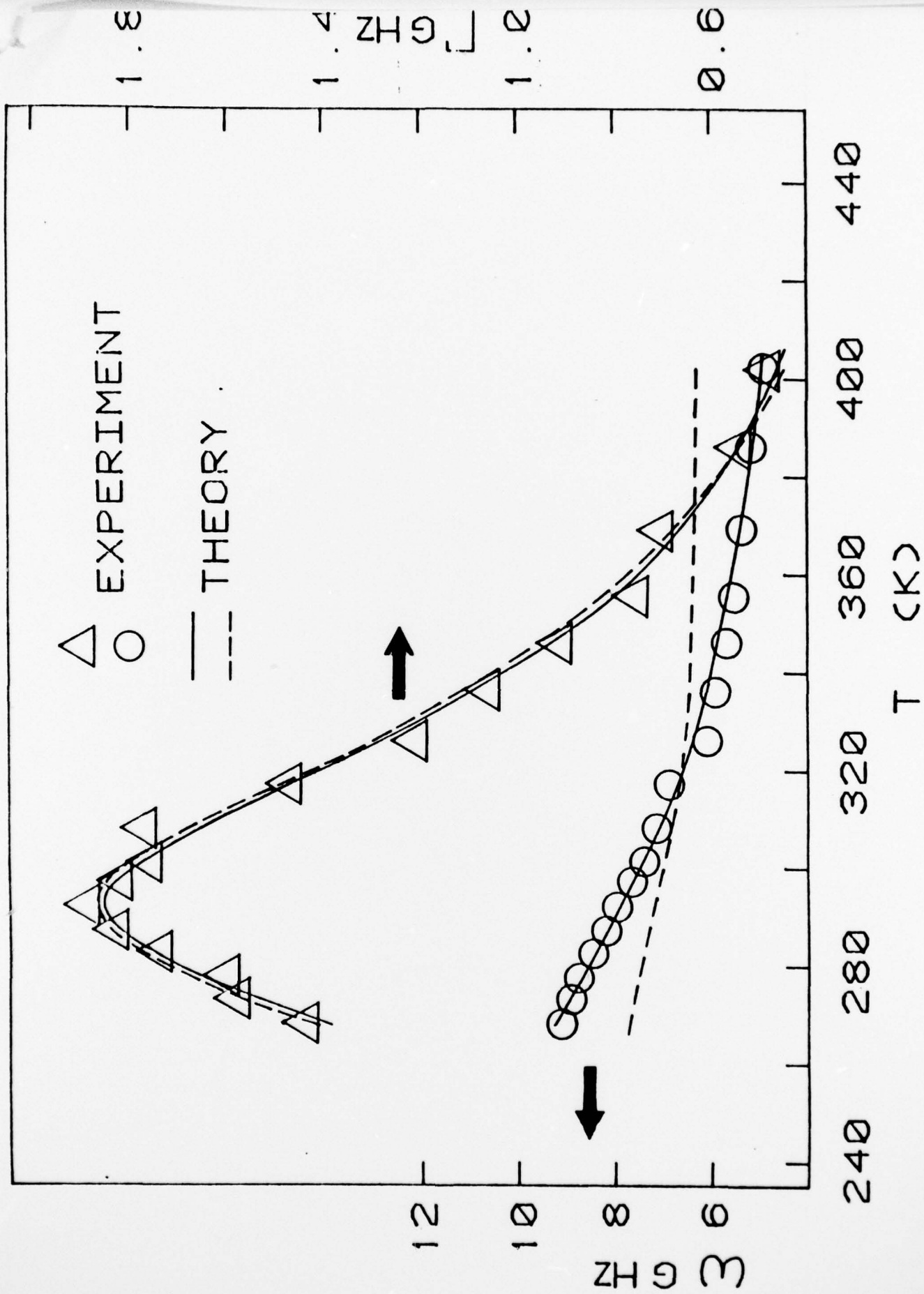
Figure 5. Comparison of the calculated and the observed Brillouin peak frequency and linewidth data as a function of temperature. The solid line is obtained for ω_q being temperature dependent; the dashed line for fixed ω_q .











No. CopiesNo. Copies

Dr. Alan Gent
Department of Physics
University of Akron
Akron, Ohio 44304 1

Mr. Robert W. Jones
Advanced Projects Manager
Hughes Aircraft Company
Mail Station D 132
Culver City, California 90230 1

Dr. C. Glori
IIT Research Institute
10 West 35 Street
Chicago, Illinois 60616 1

Dr. M. Litt
Department of Macromolecular Science
Case Western Reserve University
Cleveland, Ohio 44106 1

Dr. R. S. Roe
Department of Materials Science
and Metallurgical Engineering
University of Cincinnati
Cincinnati, Ohio 45221 1

Dr. L. E. Smith
U.S. Department of Commerce
National Bureau of Standards
Stability and Standards
Washington, D.C. 20234 1

Dr. Robert E. Cohen
Chemical Engineering Department
Massachusetts Institute of Technology
Cambridge, Massachusetts 02139 1

Dr. David Roylance
Department of Materials Science and
Engineering
Massachusetts Institute of Technology
Cambridge, Massachusetts 02039 1

Dr. W. A. Spitzig
United States Steel Corporation
Research Laboratory
Monroeville, Pennsylvania 15146 1

Dr. T. P. Conlon, Jr., Code 3622
Sandia Laboratories
Sandia Corporation
Albuquerque, New Mexico 87115 1

Dr. Martin Kaufmann, Head
Materials Research Branch, Code 4542
Naval Weapons Center
China Lake, California 93555 1

Dr. T. J. Reinhart, Jr., Chief
Composite and Fibrous Materials Branch
Nonmetallic Materials Division
Department of the Air Force
Air Force Materials Laboratory (AFSC) 1
Wright-Patterson Air Force Base, Ohio 45433

Dr. J. Lando
Department of Macromolecular Science
Case Western Reserve University
Cleveland, Ohio 44106

Dr. J. White
Chemical and Metallurgical Engineering
University of Tennessee
Knoxville, Tennessee 37916 1

Dr. J. A. Manson
Materials Research Center
Lehigh University
Bethlehem, Pennsylvania 18015 1

Dr. R. F. Helmreich
Contract RD&E
Dow Chemical Co.
Midland, Michigan 48640 1

TECHNICAL REPORT DISTRIBUTION LIST

No. Copies

No. Copies

Dr. Stephen H. Carr
Department of Materials Science
Northwestern University
Evanston, Illinois 60201

1

Dr. M. Broadhurst
Bulk Properties Section
National Bureau of Standards
U.S. Department of Commerce
Washington, D.C. 20234

2

~~Dr. G. H. Wang~~
~~Department of Chemistry~~
~~University of Utah~~
~~Salt Lake City, Utah 84112~~

1

Dr. T. A. Litovitz
Department of Physics
Catholic University of America
Washington, D.C. 20017

1

Dr. R. V. Subramanian
Washington State University
Department of Materials Science
Pullman, Washington 99163

1

Dr. M. Shen
Department of Chemical Engineering
University of California
Berkeley, California 94720

1

Dr. V. Stannett
Department of Chemical Engineering
North Carolina State University
Raleigh, North Carolina 27607

1

Dr. D. R. Uhlmann
Department of Metallurgy and Material Science
Center for Materials Science and Engineering
Massachusetts Institute of Technology
Cambridge, Massachusetts 02139

Naval Surface Weapons Center
White Oak
Silver Spring, Maryland 20910
Attn: Dr. J. M. Augl
Dr. B. Hartman

1

Dr. G. Goodman
Globe Union Inc.
5757 North Green Bay Avenue
Milwaukee, Wisconsin 53201

1

Picatinny Arsenal
SMUPA-FR-M-D
Dover, New Jersey 07801
Attn: A. M. Anzalone
Bldg. 3401

1

Dr. J. K. Gillham
Princeton University
Department of Chemistry
Princeton, New Jersey 08540

1

Douglas Aircraft Co.
3855 Lakewood Boulevard
Long Beach, California 90846
Attn: Technical Library
CI 290/36-84
AUTO-Sutton

1

Dr. E. Baer
Department of Macromolecular Science
Case Western Reserve University
Cleveland, Ohio 44106

1

Dr. K. D. Pae
Department of Mechanics and Materials Science
Rutgers University
New Brunswick, New Jersey 08903

1

NASA-Lewis Research Center
21000 Brookpark Road
Cleveland, Ohio 44135
Attn: Dr. T. T. Serofini, MS-49-1

1

Dr. Charles H. Sherman, Code TD 121
Naval Underwater Systems Center
New London, Connecticut

1

Dr. William Risen
Department of Chemistry
Brown University
Providence, Rhode Island 02912

1

TECHNICAL REPORT DISTRIBUTION LIST

	<u>No. Copies</u>		<u>No. Copies</u>
Office of Naval Research Arlington, Virginia 22217 Attn: Code 472	2	Defense Documentation Center Building 5, Cameron Station Alexandria, Virginia 22314	12
Office of Naval Research Arlington, Virginia 22217 Attn: Code 102IP 1	6	U.S. Army Research Office P.O. Box 12211 Research Triangle Park, N.C. 27709 Attn: CRD-AA-IP	1
NR Branch Office 36 S. Clark Street Chicago, Illinois 60605 Attn: Dr. Jerry Smith	1	Naval Ocean Systems Center San Diego, California 92152 Attn: Mr. Joe McCartney	1
NR Branch Office 15 Broadway New York, New York 10003 Attn: Scientific Dept.	1	Naval Weapons Center China Lake, California 93555 Attn: Head, Chemistry Division	1
NR Branch Office 130 East Green Street Pasadena, California 91106 Attn: Dr. R. J. Marcus	1	Naval Civil Engineering Laboratory Port Hueneme, California 93041 Attn: Mr. W. S. Haynes	1
NR Branch Office 10 Market Street, Rm. 447 San Francisco, California 94102 Attn: Dr. P. A. Miller	1	Professor O. Heinz Department of Physics & Chemistry Naval Postgraduate School Monterey, California 93940	1
NR Branch Office 15 Summer Street Boston, Massachusetts 02210 Attn: Dr. L. H. Peebles	1	Dr. A. L. Slafkosky Scientific Advisor Commandant of the Marine Corps (Code RD-1) Washington, D.C. 20380	1
Director, Naval Research Laboratory Washington, D.C. 20390 Attn: Code 6100	1	Office of Naval Research Arlington, Virginia 22217 Attn: Dr. Richard S. Miller	1
Asst. Secretary of the Navy (R&D) Department of the Navy Room 4E736, Pentagon Washington, D.C. 20350	1		
Commander, Naval Air Systems Command Department of the Navy Washington, D.C. 20360 Attn: Code 310C (H. Rosenwasser)	1		